HIGH RESOLUTION NANOBUBBLE-BASED PRESSURE SENSOR FOR IN VIVO MONITORING

Xuechun Wang, Eugene Yoon, and Ellis Meng
University of Southern California, Los Angeles, California, USA

ABSTRACT

A high-resolution Parylene-based pressure sensor with nanobubbles generated, localized, and monitored in real-time was tailored for *in vivo* monitoring. Using an asymmetric electrode pair, precise picoliter-volume oxygen bubbles were electrolytically generated and confined within an open microchannel configured for electrochemical impedance monitoring. Long-lasting (>4 hours) oxygen bubbles were coupled to a digital pressure source and an optical bubble tracking system to achieve a resolution of 1 mmHg (0.13 kPa). This resolution meets accuracy requirements for monitoring intracranial pressure (ICP), with a 0-20 mmHg range. The 20× resolution improvement corresponds to the best performance for a microfabricated bubble-based pressure sensor to date.

KEYWORDS

Nanobubble, Parylene C, pressure sensor, electrolysis

INTRODUCTION

Physiological pressure monitoring is a standard of care in the treatment of many health conditions and diseases. For example, an abnormal increase in pressure can have implications on disease progression or the need for medical intervention. Pressures such as ICP, intraocular pressure (IOP), and intra-abdominal pressure (IAP) that span a relatively small pressure range require sensors that can resolve pressure changes down to 1 mmHg (Table 1). Those pressures are difficult to acquire using non-invasive methods and are most accurately tracked with implanted pressure sensors with real-time monitoring capability.

Table 1: Normal range of physiological pressures.

Type	Pressure (mmHg)
ICP	7-15 [1]
IOP	11-21[2]
IAP	5-7 [3]

For measuring ICP, there are commercial pressure sensors with catheter-tip transducers such as the Camino® fiber optic parenchymal bolted catheter and Codman MicroSensor®. Such traditional membrane-based sensors are susceptible to biofouling, fluid ingress, and ion permeation [4], all of which can affect performance. Alternate transduction methods have been investigated including bubble-based pressure sensors which are designed to be compact and operate in the body's saline environment. Bubble-based sensors measure the electrochemical response of a localized bubble produced by faradaic gas evolution. Prior work demonstrated that electrolytic bubbles could be used to track pressure but lacked sufficient resolution and sensitivity for low-pressure ranges [5-7].

This work reports advances in precise, picoliter (pL) - volume bubble generation, bubble composition control, and instrumentation that together enable high-resolution pressure tracking suitable for measuring physiological pressure within 0-20 mmHg *in vivo*.

MATERIALS AND METHODS

Sensors were fabricated using Parylene surface micromachining and included four exposed platinum electrodes within a bubble confining microchannel and an exterior exposed counter electrode (Fig.1) [8-9]. A single working electrode (230 μm^2) and the pair of counter electrodes (length: 1500 μm; width: 180 μm) shorted together formed an asymmetric electrode pair, allowing a single pL-volume O_2 or H_2 bubble to be reliably generated by controlling the amplitude and pulse duration of current passing through the electrode pair [9]. Constriction valves were located at the ends of the bubble microchannel (length: 400 μm; width: 50 μm; height: 16 μm) and designed to trap the formed bubble within the sensing region. Localization of the bubble to this region allowed the electrochemical impedance to be monitored by the sensing electrode pair located on either end of the bubble microchannel regardless of sensor orientation (Fig. 1).
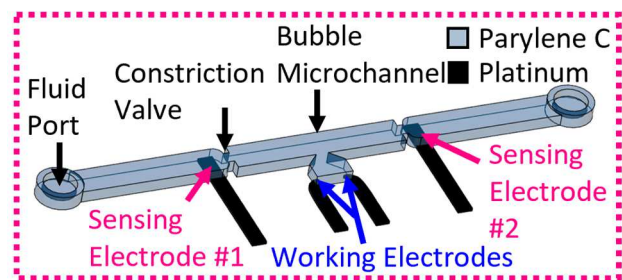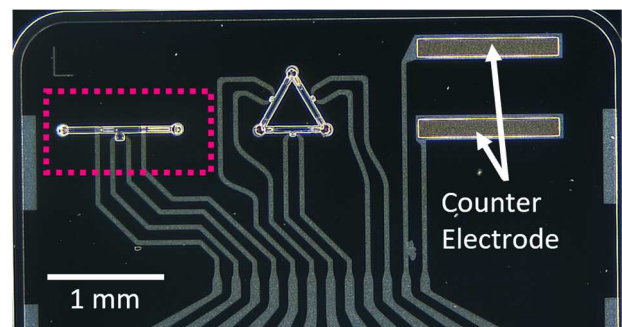

Figure 1: (Top) Micrograph of nanobubble pressure sensor with counter electrodes on a single die. Sensor is highlighted in the dotted box. (Bottom) Schematic showing sensor with major components labelled. The working and counter electrodes were used to inject current and generate the electrolytic bubble. Sensing electrodes tracked impedance across the bubble microchannel to transduce pressure. The constriction valves trapped the bubble in the sensing region of the microchannel.

The sensors were loaded into an acrylic testing fixture filled with 1× phosphate-buffered saline (PBS, to mimic the composition of physiological fluids). This system was then primed with pressurized nitrogen gas (~200 torr) overnight to fill the microfluidic channels with 1× PBS. Bubble size and shape were monitored using a microscope and Matlab script. At the same time, an LCR meter acquired impedance (at 10 kHz). Pressure sensing experiments utilized a Fluigent pressure source capable of imposing precise 1 mmHg steps (Fig. 2) over the 0-20 mmHg physiologically relevant range.
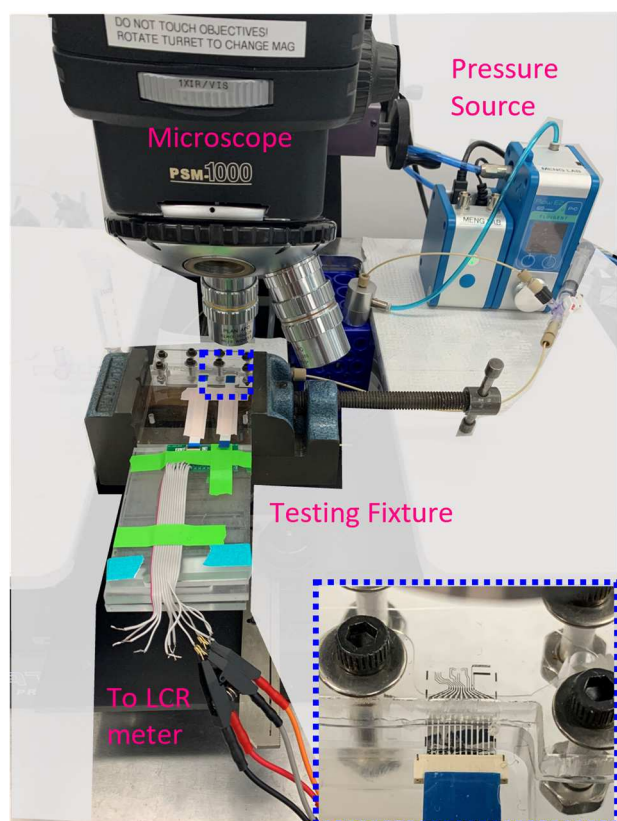

Figure 2: Photograph of testing setup with the sensor testing fixture, microscope, and Fluigent pressure source. Inset shows a close-up of the sensor in the testing fixture positioned under the microscope.

RESULTS AND DISCUSSION
Electrochemical Characterization

Sensing electrode pair were first characterized using electrochemical impedance spectroscope (EIS) measurements taken with a potentiostat. The sensor electrode-electrolyte interface can be modeled by the Randles circuit (Fig. 3). The measurement frequency of the sensor (10 kHz) was selected when the electrochemical impedance response is dominated by the solution resistance (phase ≈ -20°; Fig. 3) [6].

Bubble Generation

High-resolution and real-time pressure sensing require careful control of bubble life and size. To conserve power for *in vivo* applications, bubbles were generated using current pulses. A pL volume bubble was reliably generated using the asymmetric electrode pair and by controlling the magnitude and duration of the current pulse. A bubble of either H_2 or O_2 could be selected by applying a negative or positive current at a single working electrode, respectively.
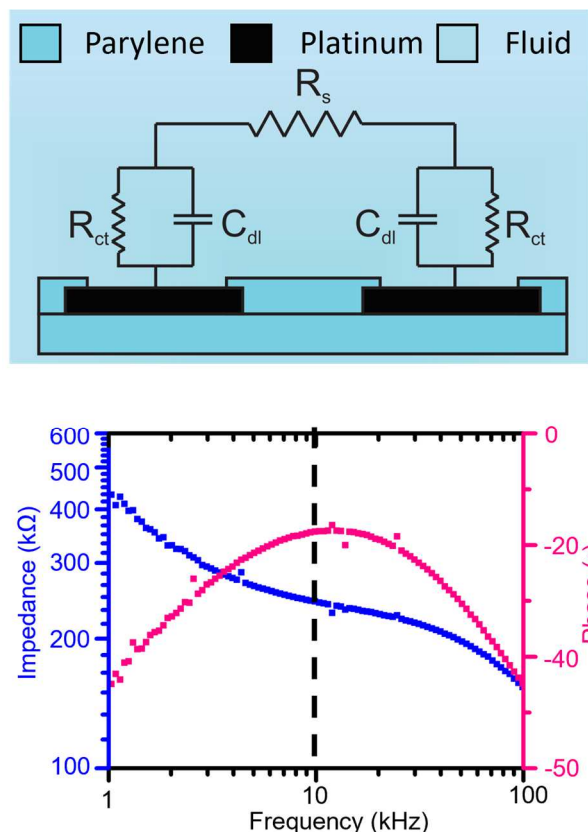

Figure 3: (Top) Randles equivalent circuit model of sensing electrode-electrolyte interface. (Bottom) Impedance and phase of the sensing electrodes. The measurement frequency (dashed line) is selected when the response is dominated by solution resistance.

Pressure Sensing

Generated bubbles gradually dissolve back into solution. Therefore, bubble lifetime impacts sensor performance. O_2 bubbles were used for pressure sensing as they lasted over three times longer, which is attributed to the lower diffusion coefficient at room temperature (Table 2; Fig. 4) [7][10].

Table 2: Diffusion coefficients of gas-liquid mixtures at 25 °C.

Solute-solvent mixture	Diffusion coefficient (cm^2/s)
H_2-H_2O	4.5×10^{-5}
O_2-H_2O	2.1×10^{-5}

48

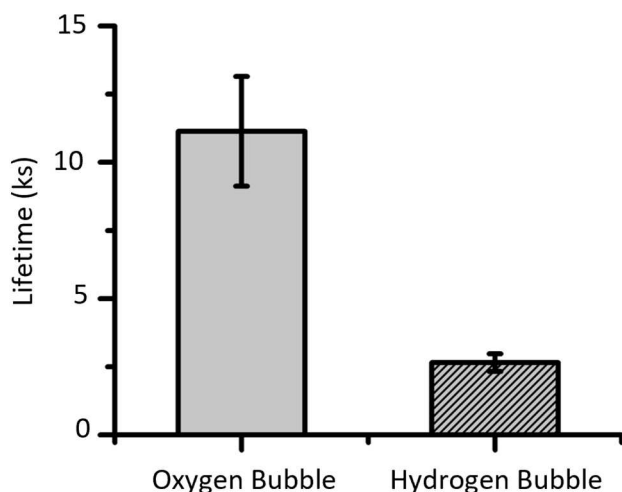*Figure 4: Lifetime of electrolytically generated O_2 (0.4 µA, 8s) and H_2 (-0.4 µA, 8s) bubbles in the microchannel after the current pulse was terminated (n=5, mean ± SD).*
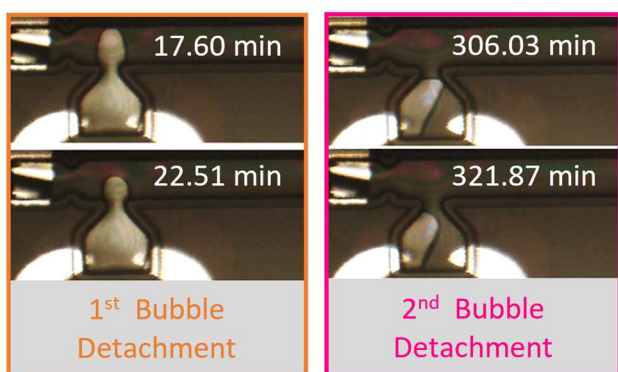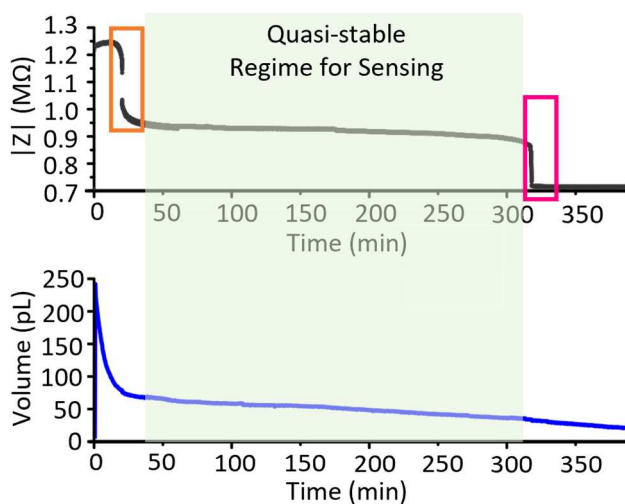

Figure 6: Maximum generated O_2 bubble size for a current pulse of +0.1 µA over 10, 15, 20, and 25 s as viewed under a microscope. Frames were processed and analyzed using Matlab script to calculate bubble volume.

Figure 5: (Top plot) Impedance response measured by sensing electrodes (black) and (bottom plot) O_2 bubble volume tracked by video feed from microscope (blue) after applied current pulse (0.3 µA, 25s). Impedance magnitude decreased as the bubble dissolved back into solution. (Bottom panels) Frame captures of bubble detachment from channel surfaces correspond to the dramatic impedance drops observed at ~20 and ~320 minutes.
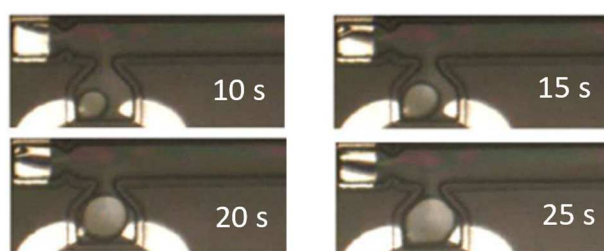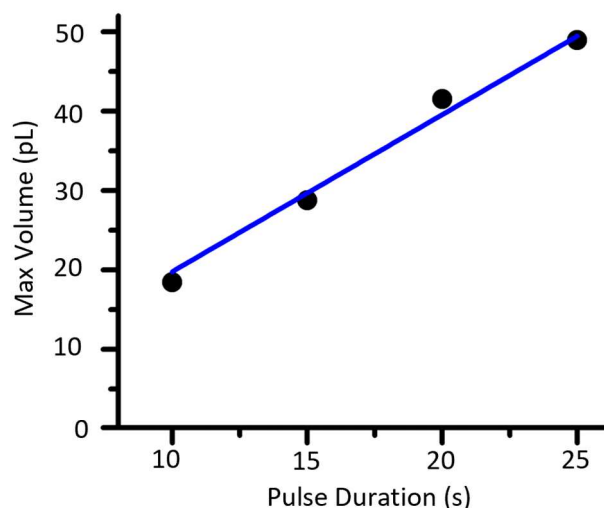
As the positive current pulse was applied, the bubble volume increased, reaching peak volume before the current pulse terminated, and then the bubble volume decreased as it dissolved back into solution. Concurrently, measured impedance followed a similar trend but with significant drops corresponding to bubble detachment from the channel wall (at 22.51 and 321.87 minutes in Fig. 5).

The quasi-stable regime of the sensor for pressure sensing was restricted during the period between major bubble detachment events (Fig. 5). The peak bubble volume was controlled in the pL range by the pulse duration (Fig. 6). Bubble volume was tracked and compared using the same applied current but varying the pulse duration (10, 15, 20, and 25 s). Bubble volume increased linearly with pulse duration (y = 1.98x, R^2 > 0.99).

To ensure linear sensor response during operation, bubbles filling the channel were generated. Real-time pressure sensing at 1 mmHg resolution was achieved over the range of 0 to 20 mmHg (Fig. 7). A linear trend was observed with a sensitivity of -82.64 Ω/mmHg (R^2>0.99; Fig. 8). This represents a 20× improvement in resolution over prior work and meets requirements for *in vivo* clinical pressure sensing.

The pressure measurement setup relies on a Keithley source meter for applying current pulse and a bulky LCR meter for measuring the impedance for pressure transduction. The future work will focus on miniaturizing

49

the measurement electronics for portability. The acrylic mold will be substituted with a Luer lock package for integration with the external ventricular drainage system for testing in the animal model for intracranial pressure monitoring.
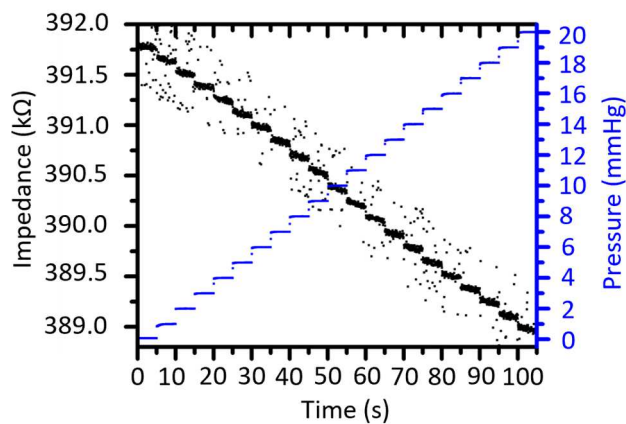

Figure 7: Sensor impedance response closely matched the 1 mmHg applied pressure steps between 0 and 20 mmHg (5 s each step).
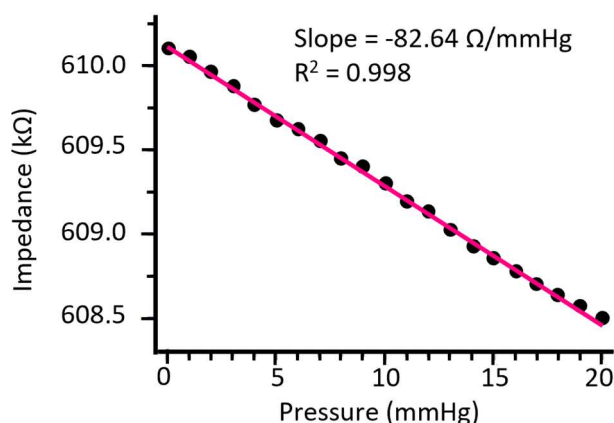

Slope = -82.64 Ω/mmHg
$R^2 = 0.998$

Figure 8: Representative curve showing a linear relationship between impedance and applied pressure with a sensitivity of -82.64 Ω/mmHg.

CONCLUSION

This work demonstrated a nanobubble-based sensor capable for transducing physiological pressure in the range 0-20 mmHg with a resolution of 1 mmHg. The bubble volume was precisely controlled in the pL scale by changing the applied current pulse duration. A quasi-stable regime for pressure sensing was determined and lasts over 4 hours for high-resolution pressure sensing with a sensitivity of 82.64 Ω/mmHg. The built-in constriction valve trapped the bubble in the microfluidic channel regardless of the sensor orientation. It shows the potential for pressure monitoring at different postures for *in vivo* applications.

REFERENCES

[1] M. Czosnyka, J. D. Pickard, "Monitoring and interpretation of intracranial pressure", *J. Neurol. Neurosurg. Psychiatry,* vol. 75, no. 6, pp. 813-821, 2004.

[2] T. Eysteinsson, F. Jónasson, H. Sasaki, A. Arnarsson, T. Sverrisson, K. Sasaki, and E. Stefánsson, "Central corneal thickness, radius of the corneal curvature and intraocular pressure in normal subjects using non-contact techniques: Reykjavik Eye Study", *Acta ophthalmologica Scandinavica,* vol. 80, pp. 11-5, 2002.

[3] B. L. De Keulenaer, J. J. De Waele, B. Powell, and M. L. N. G. Malbrain, "What is normal intra-abdominal pressure and how is it affected by positioning, body mass and positive end-expiratory pressure?", *Intensive Care Med.,* vol. 35, no. 6, pp. 969-976, 2009.

[4] L. Yu, B. J. Kim, E. Meng, "Chronically implanted pressure sensors: Challenges and state of the field", *Sensors*, vol. 14, no. 11, pp. 20620–20644, 2014.

[5] C. A. Gutierrez, E. Meng, "A subnanowatt microbubble pressure sensor based on electrochemical impedance transduction in a flexible all-parylene package", *MEMS '11 Conference*, pp. 549-552.

[6] L. Yu, E. Meng, "A microbubble pressure transducer with bubble nucleation core", *MEMS '14 Conference*, pp. 104-107.

[7] L. Yu, C. A. Gutierrez, E. Meng, "An Electrochemical Microbubble-Based MEMS Pressure Sensor", *J. Microelectromechanical Syst.*, vol. 25, no. 1, pp. 144–152, 2016.

[8] E. Yoon, E. Meng, "Electrolytic Generation of Trapped Nanobubbles via Nucleation Core with Picoliter Precision", MEMS '20 Conference, pp. 1064-1067, 2020.

[9] E. Yoon, E. Meng, " Asymmetric Microelectrodes for Nanoliter Bubble Generation via Electrolysis", *J. Microelectromechanical Syst.*, 2021.

[10] P. S. Epstein, M. S. Plesset, "On the Stability of Gas Bubbles in Liquid-Gas Solutions", *J. Chem. Phys.,* vol. 18, no. 11, pp. 1505-1509, 1950.

CONTACT

*X. Wang, tel: +1-213-8213897; xuechunw@usc.edu
*E. Meng, tel: +1-213-8213949; ellismen@usc.edu